Digitally Implemented Average Current Mode Control in Discontinuous-Conduction-Mode PFC Rectifier

Jong-Won Shin, and Bo-Hyung Cho

School of Electrical Engineering and Computer Science, Seoul National University, Seoul, 151-744, Korea

nf84@snu.ac.kr

***Abstract* — This paper proposes a digital average current mode control method in discontinuous conduction mode (DCM) power factor correction (PFC) rectifier. The proposed control technique does not estimate but directly senses the average value of the inductor current in each switching cycle. It is implemented by means of a conventional current sensing circuit and a microcontroller. The calculation burden of the microcontroller is the same with that of conventional two-loop controlled converter, because the additional calculation process is not required. The control method achieves lower total harmonic distortion (THD) and higher power factor (PF) than conventional one. Experimental results with 200-W prototype hardware verify the feasibility and performance of the proposed control method.**

***Keywords* — Average current mode control, digital control, discontinuous conduction mode (DCM), power factor correction (PFC), variable-duty-cycle control.**

I. INTRODUCTION

Harmonic current by various non-resistive electronic loads is known as the cause of problems such as power loss, noise, voltage distortion and reduced line utilization [1]. Especially, regulations on line current distortion in electronic devices pose a challenge for low power converters [2]. Active PFC units based on switch mode power supplies are considered as a general solution to minimize the harmonic current. They feature smaller size, higher efficiency and PF than passive PFC circuit [3].

DCM operation of active PFC rectifiers features low diode recovery loss, zero-current turn-on of main switch, and constant switching frequency. It is usually adopted in low to medium power range, i.e., under 200~300W, where the conduction losses in semiconductor devices are not dominant. As its conventional control law, open-loop control or constant duty cycle control is widely used due to its simplicity in the control scheme. The controller needs only a low-bandwidth voltage loop which dispenses with current sensing and control circuit [4]. The drawbacks of the open-loop control technique, however, are relatively low PF and high THD, especially when high line input voltage is applied [5]. Various researches have been done on the variable duty cycle control to overcome the aforementioned problems of open-loop control. One-cycle control method enables the variable duty cycle control with two resettable integrators and resistive sensing network of rectified input voltage [6]. Harmonic injection methods to achieve near-unity PF have been also reported though their analog control circuits are complicated [7]-[8]. Another variable frequency control scheme is implemented with input voltage feedforward [9]. Reference [10] digitally realized the control scheme in [9] by using multiplying and square-root operations.

On the other hand, sensing the average inductor current in DCM is not straightforward in digital control implementation. Generally, digital controllers employ one-sample-per-switching-cycle to sense the analog information. The sampling instant of the average inductor current depends not only on the on-time of switch as in continuous conduction mode (CCM) [11] but also on the on-time of diode. Sample correction method in CCM rectifier, which corrects the sampled inductor current by multiplying correction factor, has been proposed to minimize distortion at both ends of the half line period where the inductor current is temporarily in DCM [12].

An average current mode control in digitally controlled DCM PFC rectifier is suggested in this paper. The control method uses conventional sensing circuit and fixed sampling instant to achieve the variable duty cycle control. It requires same calculation burden with conventional CCM PFC rectifier and does not need any additional computation. The proposed control technique also features low THD and high PF.

The paper consists of following sections: In Section II, the mode analysis is given and the mathematical expression of properly controlled inductor current shape is derived. Section III illustrates experimental results with 200W prototype hardware such as oscillograms and measured THD data. The paper is summarized and concluded in Section IV.

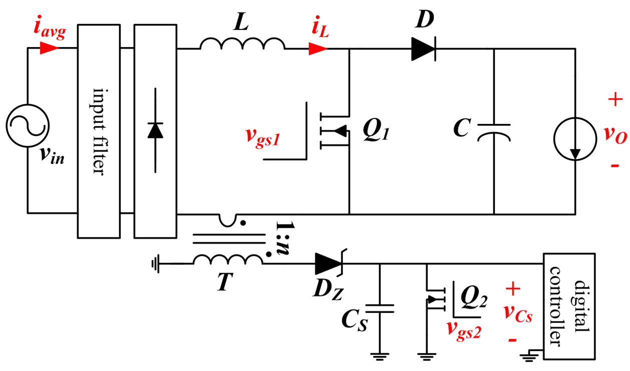

Figure 1. Proposed current control circuit with boost rectifier.

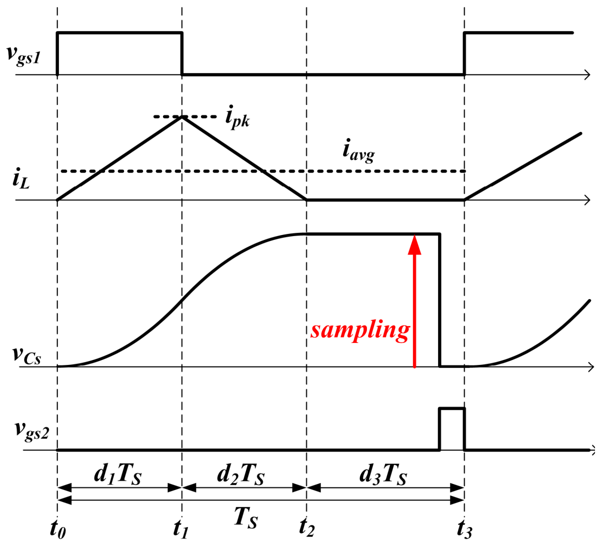

Figure 2. Operational waveforms of the proposed current control technique.

II. PROPOSED CONTROL TECHNIQUE

A. Operational Mode Analysis

A circuit diagram of a boost rectifier with proposed control technique is shown in Fig. 1. Rectified input and output voltage sensing networks and gate driver are omitted for clarity. The rectifier operates in DCM with fixed frequency and fixed sampling instant. The current sensing circuit which consists of current sensing transformer T, zener diode D_Z, sensing capacitor C_S, and reset switch Q_2 is the same as that in conventional control [13]-[14]. The digital controller controls the gate signals of the two switches Q_1 and Q_2.

The operation of the current sensing circuit is different from the conventional one in two ways: First, the gate signal of Q_2 is not complementary to that of the main switch Q_1. The turn-on instant of Q_2 is delayed until the inductor current becomes zero thus the sensing capacitor voltage v_{Cs} remains constant. After v_{Cs} is sampled by the digital controller, Q_2 turns on to discharge C_S. Second, the turn-off of Q_1 is controlled by a current loop in the average current mode control.

The operational waveforms are illustrated in Fig. 2. v_{gs1}, i_L, v_{Cs} and v_{gs2} are gate signal of Q_1, inductor current, sensing capacitor voltage, and gate signal of Q_2 respectively. Unit switching period is separated in three modes to explain the operation of the proposed current control. Time segments d_1T_S and d_2T_S represent the on-time of Q_1 and output diode D respectively. To simplify the analysis, semiconductor devices are assumed to be ideal. Rectified input voltage $|v_{in}|$ and output voltage v_O are also approximated to be constant within a switching period.

- Mode 1 [t_0~t_1]: At t_0, Q_1 turns on by the fixed frequency signal of the digital controller. i_L linearly increases with the slope $\frac{|v_{in}|}{L}$, where L is inductance of boost inductor. Then the current sensing transformer T outputs the scaled inductor current through D_Z to C_S. $v_{Cs}(t)$ is shown in (1).

$$v_{Cs}(t) = \frac{1}{nC_S}\int_{t_0}^{t} i_L(t)dt \quad (1)$$

n represents the turn number of secondary winding of T. $v_{Cs}(t)$ increases in parabolic way from zero because the rectifier operates in DCM.

- Mode 2 [t_1~t_2]: When Q_1 turns off at t_1 by the current loop, i_L decreases with the slope $\frac{v_O-|v_{in}|}{L}$. $v_{Cs}(t)$ still increases but the sign of the parabolic curve is inverted.
- Mode 3 [t_2~t_3]: After t_2, i_L maintains zero and $v_{Cs}(t)$ remains constant as in (2):

$$v_{Cs}(t) = \frac{T_S}{nC_S}\left[\frac{1}{T_S}\int_{t_0}^{t} i_L(t)dt\right] = \frac{T_S}{nC_S}\left[\frac{1}{T_S}\int_{t_0}^{T_S} i_L(t)dt\right] = \frac{T_S}{nC_S} i_{avg}, \quad (2)$$

where T_S is the switching period and the term in the braces is the average inductor current in a switching cycle or i_{avg}. In this interval, $v_{Cs}(t)$ represents the average inductor current because i_L in Mode 1 and Mode 2 is fully integrated. The digital controller then triggers the internal ADC to sample the $v_{Cs}(t)$ to compare it with the inner loop current reference. After the sampling, Q_2 turns on

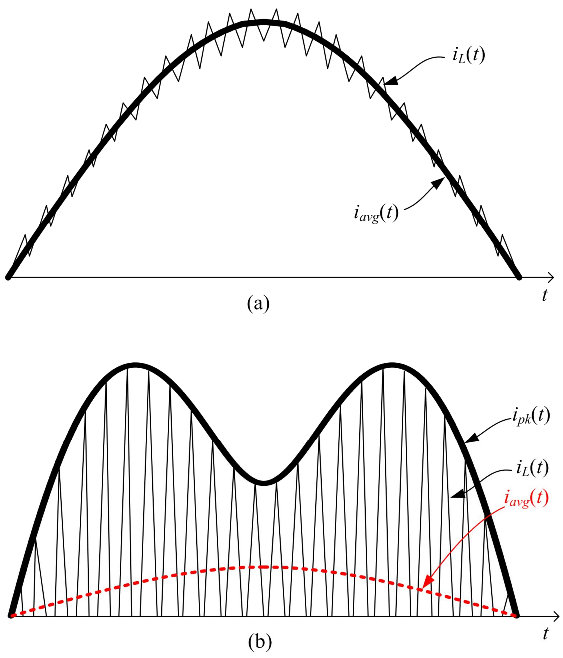

Figure 3.Comparison of inductor current shapes between (a) CCM and (b) DCM rectifier.

to discharge C_S before the next turn-on signal of Q_1 occurs. Because the sampling instant is fixed in unit switching cycle, the digital controller does not spend any resource to determine when the sampling should occur in each switching cycle.

B. Inductor Current Shaping

Generally, the inductor current waveform of average current mode controlled CCM boost rectifier resembles the sinusoid of the input voltage to achieve high PF and low THD. However, unlike in CCM rectifier, the envelope of the inductor current in DCM rectifier does not look like a sinusoid. Fig. 3 compares the current shapes in general CCM and DCM PFC rectifier over half line period. The envelope of the inductor current of DCM PFC, $i_{pk}(t)$, does not follow the sine wave though its average value per switching cycle, $i_{avg}(t)$, tracks sine wave as in Fig. 3(b).

If the average inductor current per switching cycle is controlled to be proportional to the sinusoidal input voltage, $i_{pk}(t)$ can be derived from the duty ratios d_1 and d_2 as in (3) and (4):

$$d_1 = \frac{Li_{pk}(t)}{v_{in}(t)T_S},\ d_2 = \frac{Li_{pk}(t)}{\left(v_O - v_{in}(t)\right)T_S}. \qquad (3), (4)$$

$i_{avg}(t)$ is derived from the geometry of the waveform shown in Fig. 2 with unknown constant X as shown in (5).

$$i_{avg}(t) = \frac{1}{2}(d_1 + d_2)i_{pk}(t) = X\sin\omega_L t \qquad (5)$$

$v_{in}(t)$ is assumed to be the pure sine wave with peak value V_{pk} and period $T_L = \frac{2\pi}{\omega_L}$ which is expressed in (6).

$$v_{in}(t) = V_{pk}\sin\omega_L t \qquad (6)$$

Substituting (3), (4) and (6) into (5) yields (7).

$$i_{pk}(t) = \sqrt{\frac{2T_S V_{pk} X}{L}}\sqrt{1 - \frac{V_{pk}\sin\omega_L t}{v_O}}\sin\omega_L t \quad (7)$$

The unknown constant X can be derived from input

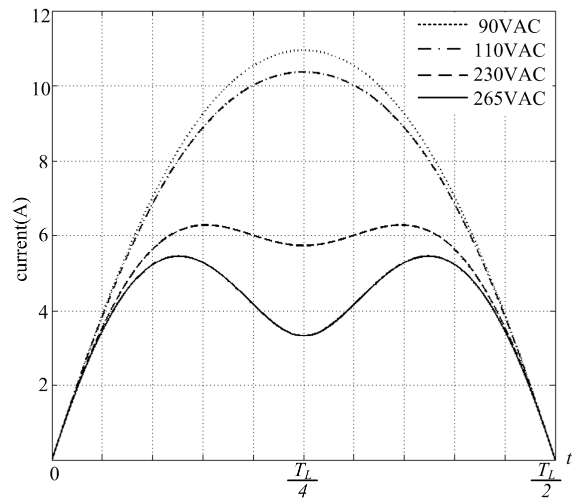

Figure 4. Inductor current envelopes for various line voltages and 200W load in average current mode DCM rectifier.

TABLE I. CIRCUIT PARAMETERS OF LABORATORY PROTOTYPE

Device		Parameter
Power Component	L	70µH
	C	220nF/450V electrolytic
	Q_1	STW20NM50
	D	FSF10A60
Current Sensing Circuit	T	turns ratio 1:50
	D_Z	1N4744
	C_S	220nF/50V ceramic
Digital Controller	Part name	dsPIC33FJ16GS502
	Switching/sampling frequency	65kHz
	Number operation	Q15 method based on fractional data type
	ADC resolution	10 bits
	K_{adc}	0.3
	FM	2.2245

power consideration. If P_{in}, P_O and η are the input power, output power, and efficiency of the rectifier system, i.e., input filter and rectifier, (8) can be achieved.

$$P_{in} = \frac{P_O}{\eta} = I_{rms}V_{rms} = \frac{1}{2}V_{pk}X \qquad (8)$$

I_{rms} and V_{rms} in (8) represent rms value of the input current i_{avg} and the input voltage v_{in} respectively. Rearranging and substituting (8) into (7) finally yields (9).

$$i_{pk}(t) = 2\sqrt{\frac{T_S P_O}{\eta L}}\sqrt{1 - \frac{V_{pk}\sin\omega_L t}{v_O}}\sin\omega_L t \qquad (9)$$

Fig. 4 illustrates the inductor current envelopes for various line input voltages and 200W load. The current envelope shows a “saddle” in the middle of the half line period. It is because the term in the second square root in (9) is not a constant but a function of $\sin\omega_L t$. The performance improvement between the proposed and the conventional current control techniques is emphasized when high line voltage is applied because the saddle is deeper at higher line voltages.

III. EXPERIMENTAL RESULTS

The proposed current control technique is verified by 200W laboratory prototype circuit. The circuit parameters are summarized in Table I.

The line input voltage to the prototype circuit is 60Hz 230VAC and the output voltage is controlled to be 400VDC.

Fig. 5 compares current waveforms between conventional open-loop control and the proposed variable duty cycle control at full load with same power stage. The line input current i_{avg} is the filtered version of i_L by simple second-order L-C filter as shown in Fig. 1. In Fig. 5(a),

i_{avg} in conventional control does not resemble sine wave and is distorted. However, in Fig. 5(b), saddles are observed in the inductor current envelope as explained in Fig. 4. The line input current of the proposed control scheme is much less distorted and looks like sinusoid.

Measured harmonic components of two control methods at 75% load are 31.9% (conventional) and 14.9% (proposed). The proposed control outperforms the conventional control by obtaining lower THD and higher PF.

IV. CONCLUSION

An average current control method for digital DCM PFC rectifier has been proposed. The control method achieves lower current distortion by employing a conventional sensing circuit method than conventional open-loop control method. Operational modes, current shaping, and rectifier design procedure have been analyzed and explained with mathematical expressions. The proposed control technique has been verified and compared with conventional one by experimental results of 200W a prototype system. Waveforms and measured data have proved that the proposed control with average current sensing and sampling technique achieves lower line current distortion.

V. ACKOWLEDGEMENT

This work was partially supported by "the New and Renewable Energy Program of the Korea Institute of Energy Technology Evaluation and Planning (KETEP) grant" funded by the Korea government Ministry of Knowledge Economy (No. 10035491, 20104010100490).

REFERENCES

[1] K. Billings, "Switchmode Power Supply Handbook," 2nd Ed., McGrawHill, 1999.

[2] Limits for Harmonic Current Emissions (Equipment Input Current <16A per Phase), IEC 61000-3-2 Int. Std., 2001.

[3] O. Garcia, J. A. Cobos, R. Prieto, P. Alou, and J. Uceda, "Single phase power factor correction: a survey," IEEE Trans. Power Electron., vol. 18, no. 3, pp. 749-755, May 2003.

[4] J. Lazar and S. Cuk, "Open loop control of a unity power factor, discontinuous conduction mode boost rectifier," in Proc. IEEE Int. Telecommunications Energy Conf. (INTELEC), 1995, pp. 671-677.

[5] K. H. Liu and Y. L. Lin, "Current waveform distortion in power factor correction circuits employing discontinuous-mode boost converters," in Proc. IEEE Power Electron. Spec. Conf. (PESC), 1989, pp. 825-829.

[6] Z. Lai, K. M. Smedley and Y. Ma, "Time quantity one-cycle control for power-factor-correctors," IEEE Trans. Power Electron., vol. 12, no. 2, pp. 369-375, Mar. 1997.

[7] D. Weng and S. Yuvarajian, "Constant switching frequency ac-dc converter using second harmonic injected PWM", IEEE Trans. Power Electron., vol. 11, no. 1, pp. 115-121, Jan. 1996.

[8] D. S. Schramm and M. O. Buss, "Mathematical analysis of a new harmonic cancellation technique of the input line current in DICM boost converters," in Proc. IEEE Power Electron. Spec. Conf. (PESC), 1998, pp. 1337-1343.

[9] J. Lazar and S. Ćuk, "Feedback loop analysis for ac/dc rectifiers operating in discontinuous conduction mode," in Proc. IEEE Applied Power Electron. Conf. (APEC), 1996, pp. 797-806.

[10] Z. Z. Ye and M. M. Jovanović, "Implementation and Performance Evaluation of DSP-Based Control for Constant-Frequency Discontinuous-Conduction-Mode Boost PFC Front End," IEEE Trans. Industrial Electron., vol. 52, no.1, pp. 98-107, Feb. 2005.

[11] D. M. Van de Sype, K. De Gussemé, A. P. Van den Bossche, and J. A. A. Melkebeek, "A Sampling Algorithm for Digitally Controlled Boost PFC Converters," IEEE Trans. Power Electron., vol. 19, no. 3, pp. 649-657, May 2004.

[12] K. De Gussemé, D. M. Van de Sype, A. P. Van den Bossche, and J. A. A. Melkebeek, "Sample correction for digitally controlled boost PFC converters operating in both CCM and DCM," IEEE Trans. Power Electron., vol. 19, no. 3, pp. 649-657, May 2004.

[13] W. Tang, F. C. Lee, R. B. Ridley, and I. Cohen, "Charge Control: Modeling, Analysis, and Design," IEEE Trans. on Power Electron., vol. 8, no. 4, pp.396-403, Oct. 1993.

[14] Z. Lai, and K. M. Smedley, "A Family of Continuous-Conduction-Mode Power-Factor-Correction Controllers Based on the General Pulse-Width Modulator," IEEE Trans. on Power Electron., vol. 13, no. 3, pp.501-510, May 1998.

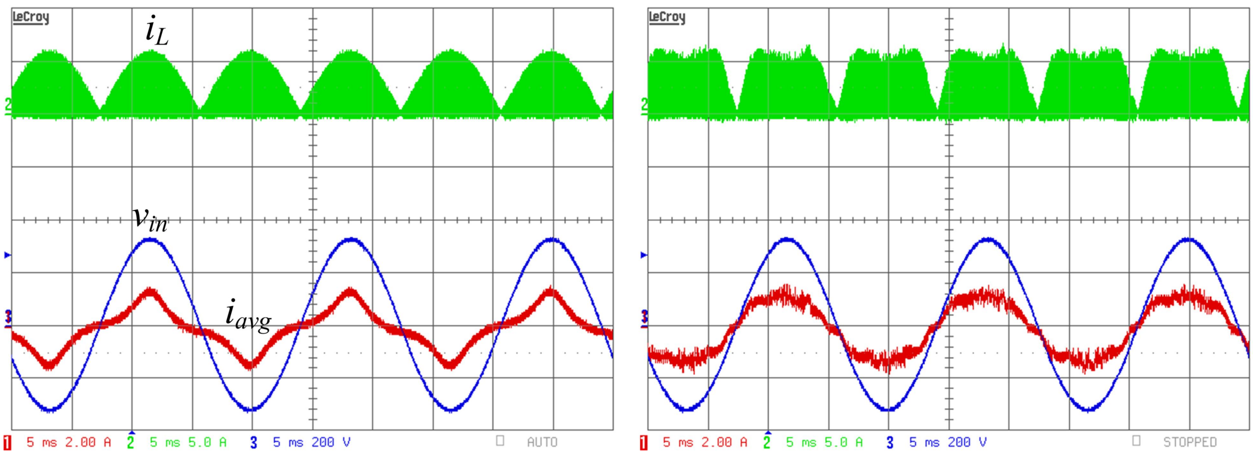

(a) (b)

Figure 5. Current waveforms comparison between (a) conventional open-loop control and (b) proposed variable duty cycle control.